

# Differential alterations in the expression of AMPA receptor and its trafficking proteins in the hippocampus is associated with recognition memory impairment the rotenone-Parkinson's disease mouse model: neuroprotective role of *Bacopa monneiri* extract CDRI 08

Vartika Gupta

Banaras Hindu University

S. Prasad (✉ [s.sprasadbhu@gmail.com](mailto:s.sprasadbhu@gmail.com))

Banaras Hindu University

---

## Research Article

**Keywords:** Parkinson's disease, recognition memory, cognition and, AMPA receptor, GluR1, GluR2, *Bacopa monnieri*, BME (CDRI-08)

**Posted Date:** January 1st, 2024

**DOI:** <https://doi.org/10.21203/rs.3.rs-3768834/v1>

**License:** © ⓘ This work is licensed under a Creative Commons Attribution 4.0 International License.

[Read Full License](#)

**Additional Declarations:** No competing interests reported.

---

# Abstract

Parkinson's disease (PD), one of the age-associated neurodegenerative disorders, is associated with motor abnormalities. In addition, the PD leads to gradual deterioration of cognitive decline with advancing age. Apart from the hallmark accumulation of  $\alpha$ -Synuclein ( $\alpha$ -Syn) in the substantia nigra pars compacta (SNPc) dopaminergic neurons leading to their loss, the precise molecular basis of the PD-induced cognitive decline and the therapeutic intervention is not yet understood. In the current study, our Western blotting and qRT-PCR data from the rotenone-induced PD mouse model reveal that the PD-induced recognition memory loss is associated with significant upregulation of the GluR1 subunit and downregulation of Glur2 subunit of the AMPA receptor in the hippocampus of rotenone-treated mice as compared to the vehicle control mice. Our data also reveal that its trafficking proteins are significantly upregulated in hippocampus (DG, CA3, and CA1 regions) of PD mice compared to the vehicle control. *Bacopa monnieri* extract (BME) called CDRI-08 at the dose of 200mg/Kg BW has shown its abilities to reverse the expression of AMPA receptor subunit and its trafficking protein in differential manner depending on whether the BME treatment was given prior to or after the rotenone treatment to mice. Our data clearly suggest that the pre treatment given to mice reverses the expression of the memory associated genes compared to the treatment after rotenone administration. Our study further suggests that the above changes in the gene expression in PD affected hippocampus are associated with modulation of their transcriptional machinery by BDNF and CREB. Expression of both are significantly lowered in the hippocampus the rotenone-treated mice in comparison to their levels in the control mice. The mice treated first with CDRI-08 significantly upregulated their expression compared to rotenone-treated mice, and when compared with mice treated after the rotenone treatment. Our results provide the evidence for the underlying molecular basis of cognitive decline in PD in rotenone-PD model and the possible mechanisms for the neuroprotective role of *Bacopa monnieri* extract CDRI-08 which shows its therapeutic potential for the PD-induced cognitive impairment.

## Introduction

Parkinson's disease (PD) is a prevalent neurological disorder that affects around 1% of the global population aged 65 years or older[1]. The aetiology of the disease is attributed to the degeneration of dopaminergic neurons in the substantia nigra pars compacta region of the midbrain, along with the aggregation of Lewy bodies composed of misfolded  $\alpha$ -Synuclein protein. PD is primarily characterised by the presence of bradykinesia, resting tremors, postural instability, and rigidity[2–4]. As the disease advances, individuals with PD may also experience non-motor features, such as impairments in executive function, memory consolidation, recalling, and processing information which leads to cognitive deficits[5–7]. Reports suggest that PD leads to dementia, referred as PD-dementia (PDD) [8–9]. However precise mechanism underlying PD-induced cognitive impairment is not fully explored. Cognition is strongly associated with neuronal plasticity which is hampered in neurodegenerative conditions[10]. Several studies going on to explore the mechanism by which synaptic plasticity is being regulated in which long-term potentiation(LTP) and long-term depression (LTD) play a crucial role [11].

The establishment of LTP which is the principal pathway for the development of learning and memory occurs in the hippocampus governed by two major ionotropic glutamate receptors;  $\alpha$ -amino-3-hydroxy-5-methyl-4-isoxazole-propionate receptor (AMPA) and N-methyl-D-aspartate receptor (NMDAR) [12–16]. The pathway is initiated by the release of glutamate from pre-synaptic neurons which activates the AMPA receptor at post-synaptic density and depolarizes the post-synaptic membrane. Depolarization of the post-synaptic membrane activates NMDAR by removing the  $Mg^{2+}$  block to achieve postsynaptic potential (PSP) which in turn allows extracellular  $Ca^{2+}$  and  $Na^{+}$  influx [17–20]. The  $Ca^{2+}$  binds to the CaMKII $\alpha$  that mediates more AMPAR and NMDAR on the postsynaptic membrane as well as activate transcription factor cAMP-response element binding protein (CREB) [21] for regulating gene expression of various synaptic plasticity-related protein such as brain-derived neurotrophic factor (BDNF) [16, 20]. BDNF play an important role in hippocampal memory formation by regulating several neuronal activities. These factors have the potential to serve as a focus for understanding PD-associated cognitive impairment and also aid in the treatment of memory decline due to PD. One of the neuromodulatory herb *Bacopa monnieri* is used in the present study to see its neuroprotective as well as neurotherapeutic role on PD.

*Bacopa monnieri*, also referred to as Bramhi is a well-known herbal plant that has been utilised in the traditional Indian medicinal system (Ayurveda) for centuries. Its extract has been employed as a nerve tonic to address a range of neurological disorders associated with memory [21–23]. *Bacopa monnieri* extract (BME) contains saponins such as bacosides, flavonoids, bacosaponines, bacoside N1 etc. [24–25]. BME has an anti-inflammatory, anti-apoptotic, antioxidative and memory-boosting role in many neurological diseases [26–28]. In the light of its nootropic effect, the present study has been designed to study the effects of *Bacopa monnieri* extract (CDRI-08) on AMPA receptor subunit; GluR1 and GluR2, its trafficking proteins and regulatory molecules (CREB and BDNF) in the hippocampus of rotenone-induced PD mouse.

## Materials and methods

### Animals

Male Swiss albino mice were inbred and confined in six per cage in an optimum temperature ( $25 \pm 1^{\circ}C$ ), photoperiods (12 hours light/dark cycle) with unrestricted access to standard mice food and water. The mice were cared under the guidelines set by the Committee for Control and Supervision of Experiments on Animals (CPCSEA). All experimental procedures were approved by the Institutional Animal Ethical Committee of Banaras Hindu University, Varanasi (Approval no.: BHU/DOZ/IAEC/2021–2022/007, Dated 15/02/2022).

### Chemicals

All chemicals utilized in the research were of analytical and molecular grades, procured from reputable suppliers such as Sigma, Merck, SRL, and Qualigens India. The primary antibodies used in this study were  $\alpha$ -Synuclein, GluR1, GluR2, post-synaptic density-95 (PSD95), transmembrane AMPA receptor regulatory

protein (TARPy-2), and protein interacting with C Kinase-1 (PICK-1). These antibodies were procured from DSHB, Peprotech, Bioss, Neuromab UC and Davis, USA. The secondary antibody used was HRP-conjugated (Genie, Bangalore, India) and Fluorophores tagged (AbCam, USA). The standardized extract of *Bacopa monnieri* Extract (BME)-CDRI-08, was graciously provided by Dr. H. K. Singh (former Director, CDRI, Lucknow, India). CDRI-08 contains approximately  $55 \pm 5\%$  of Bacosides A and B.

## Grouping, Drug preparations and administration

The mice were divided into four groups, each consisting of nine mice. The groups were as follows: (1) Control group, which received dimethyl sulfoxide (DMSO) subcutaneously for 14 days, and after that 5% Tween 80 was given orally; (2) Rotenone Treated group, which received 2mg/kg BW Rotenone dissolved in DMSO subcutaneously for 14 days; (3) Rotenone pre-treated with *Bacopa monnieri* extract (BME) group, which received 200mg/kg BW of BME dissolved in 5% tween 80 orally for 21 days before administration of Rotenone; and (4) Rotenone post-treated with *Bacopa monnieri* extract (BME) group, which received 200mg/kg BW of BME dissolved in 5% tween 80 orally for 21 days after administration of Rotenone. After the completion of treatments, a behaviour evaluation was conducted and subsequently, the mice were sacrificed, followed by decapitation. The hippocampus was then isolated for RNA isolation and protein homogenate preparation for qPCR and western blotting. The brain was stored for the cryosection for IFC.

## Grip-strength Test

The grip-strength test was conducted using a Medcraft grip-strength meter to evaluate the maximal muscle strength of the forelimbs in mice. Each mouse was gently grasped by the tail and allowed to hold onto the horizontal bars that were linked to the sensor. The mouse was subjected to a retrograde force, and the maximum force exerted by the animal was measured in kg. Each mouse underwent the identical treatment three times[29].

## Rotarod Test

The rotarod test involved placing mice on a rotating rod. The rotational speed of the standard testing apparatus was increased from 5 to 15 revolutions per minute (rpm) for 120 seconds per mouse for three consecutive days. On the fourth day, the time it took for each mouse to fall off the spinning rod (referred to as latency) was measured and recorded[30].

## Novel Object Recognition Test

Novel object recognition (NOR) test is comprised of habituation, training, and tests task. Mice were habituated in a 50cm × 50cm × 40cm open field for 5 minutes without objects. After 24 hours of habituation, training began. Two similar-shaped and sized objects were placed in an open field. The mice were then introduced one by one into the open field for 5 minutes and recorded while they explored the two objects. The training was done twice in 28 hours. Test sessions were conducted 48 hours after the last training session by replacing a familiar object with a novel one. Mice were then placed in the box and allowed to explore for 5 minutes, which was recorded. ANY-maze software (version 7.2, Stoelting Co.,

USA) was used to analysing the videos. Mouse interaction with objects is measured by mouse head entry in the periphery. Time spent with the novel object was calculated as  $T_{\text{Novel}}/(T_{\text{Novel}} + T_{\text{Familiar}})$ , time spent with the familiar object was calculated as  $T_{\text{Familiar}}/(T_{\text{Novel}} + T_{\text{Familiar}})$ , and Discrimination Index (DI) for the novel object was calculated as  $(T_{\text{Novel}} - T_{\text{Familiar}})/(T_{\text{Novel}} + T_{\text{Familiar}})$  [31].

## Western blot analysis

To check the expression of proteins, the hippocampus was mechanically homogenized in RIPA buffer containing 150 mM NaCl, 2 mM EDTA, 50 mM Tris-HCl (pH 7.4), 1% Triton X-100, 0.5% sodium deoxycholate, 0.1% SDS, PMSF and protease inhibitor cocktail. The protein concentration of the sample was assessed by the Bradford reagent [32]. The proteins of different groups were separated by SDS-PAGE [33] and transferred onto a PVDF membrane by wet transfer method. The membrane was blocked in blocking solution (5% non-fat skimmed milk in TBST) for 3 hours at room temperature, the membranes were then incubated overnight with their respective primary antibodies  $\alpha$ -Synuclein (DSHB-S1-890 H3C-s-Supernatant), GluR1 (DSHB-S1-1880, N355/1-supernatant), GluR2(DSHB-S1-1881, L21/32-supernatant), Anti-PICK-1(UC-Davis-Neuromab, L20/8), anti-PSD-95(UC-Davis-Neuromab, K28/43), CREB (Bioss, bs-0036R) and BDNF (Peprotech, 500P-84). Thereafter membranes were washed in TBST and incubated in appropriate HRP-conjugated secondary antibodies at a dilution of 1:2000 (Genei Laboratories, India). The membrane was washed in TBST, and signals were detected using the ChemiDoc imager (AI680) by ECL method. As an internal control for normalization, the same blot was stripped and probed with an anti- $\beta$  actin HRP-conjugated antibody (Sigma, A3854). Blots were scanned and quantified by AlphaEase FC (Alphamager 2200) software.

## qRT- PCR (quantitative reverse transcription PCR)

To check the expression of GluR1 (*GRIA-1*) and GluR2 (*GRIA-2*) at the transcript level qRT-PCR was done. To carry out this first RNA was isolated using TRI reagent (Sigma- Aldrich, USA) [34] and cDNA was synthesized taking 5 $\mu$ g RNA. Amplification was done using cDNA as template DNA with specific primers and PowerUp SYBR Green master mix (Thermo Fisher Scientific, USA) for GluR1 (F- 5'GAACGAAGGACTGTCAACATG3'; R-5'AGAGCTTCCTGTAGTTCCG3') and GluR2 (F- 5'CAGTGCATTTCCGGTAGG3'; R- 5'TTGGTGACTGCGAAACTG3').  $\beta$ -actin (F- 5'ATCGTGGGCCGCTCTAGGCACC3'; R- 5'CTCTTTGATGTCACGCACGATTTTC3') as endogenous control was used for normalization. The relative fold change in gene expression was calculated using the  $2^{-\Delta\Delta CT}$  method [35].

## Immunofluorescence (IFC)

To check the expression of  $\alpha$ -Synuclein, GluR1 and GluR2 in hippocampal subregions, IFC was performed according to Dalvi and Belsham[36]. Initially, the brain was transcardially perfused with 4% paraformaldehyde (PFA) to fix the brain, after completion of perfusion brain tissue was incubated in 4% PFA overnight. Then brain was cryopreserved with a different gradient of sucrose solution (10%, 20%, and 30%). Then the tissue was embedded in OCT and coronal sections (10  $\mu$ m thick) were obtained using a

cryostat (Leica Biosystem, Germany). These sections were then affixed onto slides that had been coated with poly-L-lysine. The cryosections were incubated for one hour at 37°C until the water evaporated. To remove the cryomount, the dried sections were washed three times in 1XPBS buffer (2.7 mM KCl, 137 mM NaCl, 4.0 mM KH<sub>2</sub>PO<sub>4</sub>, 4.3 mM Na<sub>2</sub>HPO<sub>4</sub>, pH 7.4) for five minutes each. Sections were permeabilized for 40 minutes with 1% TritonX-100 in 1X PBS buffer, then washed with the same buffer to remove excess TritonX-100. Following that, sections were treated for 2 hours with 5% normal goat serum (NGS) to suppress nonspecific proteins. In a humidity chamber, sections were treated overnight with diluted  $\alpha$ -Synuclein (DSHB-S1-890H3C-s-Supernatant), GluR1 (DSHB-S1-1880 N355/1-supernatant), and GluR2 (DSHB-S1-1881 L21/32-supernatant), primary antibody (0.5 $\mu$ g/ $\mu$ l in 2% NGS-1X PBS solution). The next day, following three 1X PBS washing at room temperature sections were then treated for 2 hours at room temperature in the dark with FITC (for  $\alpha$ -Synuclein) and TRITC (for GluR1 & GluR2)-labelled goat anti-mouse anti-IgG secondary antibodies at 1:250 dilution in 2% NGS-1X PBS buffer. The sections were then washed in 1X PBS buffer, treated with DAPI for 10 minutes at room temperature, and mounted with an anti-fade mounting solution containing DABCO and glycerol. By omitting the primary antibody, a negative control slide was also made to identify the non-specific signals. Photomicrographs were taken at 40X magnification using a Laser scanning super-resolution microscope (Confocal microscope). The immunofluorescence signal for  $\alpha$ -Synuclein, GluR1 and GluR2 expression was evaluated using ZEISS ZEN blue software Area integrated density measuring tool.

## Statistical analysis

The data acquired from the behavioral analysis, qRT-PCR, western blotting, and immunofluorescence chemistry (IFC), were statistically analysed by One-way analysis of variance (ANOVA) followed by Tukey's post-hoc test after performing the Shapiro-Wilk normality test. The values are represented as mean  $\pm$  SEM. Statistical analysis was conducted with SPSS 16.0 for Windows, and  $p < 0.05$  indicating statistical significance.

## Results

### Effect of BME on altered motor behavior in PD mice

The neuromuscular and skeletal strength of mice is evaluated using a method called the grip-strength test. As seen in Fig. 1A, the treatment of rotenone resulted in a significant ( $p < 0.05$ ) reduction in the grip strength of PD mice as compared to the group that served as the control. However, mice that were post-treated with BME had a significant ( $P < 0.05$ ) rise, although to a lesser extent than mice that were pre-treated with BME. The effects of BME pretreatment on mice had more potential to suppress these effects. Furthermore, rotarod test locomotion and balance showed that mice with rotenone-induced Parkinson's disease spent much less time ( $P < 0.05$ ) on the revolving rod compared to the control group. When comparing mice that were pre-treated and post-treated with BME, it was observed that the mice spent a significantly longer length on the revolving rod, which suggests an improvement in their motor behavior. Nevertheless, the mice that received pre-treatment of BME exhibited a more noticeable impact compared

to the mice that received post-treatment of BME, when compared to the mice with Parkinson's disease (Fig. 1B).

## **Effect of BME on $\alpha$ -Synuclein expression alteration due to PD**

The level of  $\alpha$ -Synuclein expression is significantly elevated ( $P < 0.05$ ) in mice affected with Parkinson's disease in comparison to mice in the control group. Nevertheless, the PD mice that received pre- and post-BME treatment exhibited a significant reduction in the expression of altered  $\alpha$ -Synuclein compared to the normal control mice (Fig. 2A-B). Furthermore, immunofluorescence labelled immunohistochemistry (IHC) in the Dentate Gyrus (DG), Cornu Ammonis-3 (CA3), and Cornu Ammonis-1 (CA1) regions of the hippocampus in brain slices (Fig. 2C-H) showed a comparable pattern to that reported in the Western blot analysis data. In brief, the expression level of  $\alpha$ -Synuclein is significantly elevated in the DG, CA3, and CA1 areas of the hippocampus in PD mice when compared to control mice. The administration of BME before and after therapy in PD mice resulted in significant amelioration of  $\alpha$ -Synuclein levels. However, the immunohistochemistry (IHC) data indicates that the pre-treatment has a much greater amelioration capability compared to the post-BME treatment.

## **Effect of BME on altered recognition memory in PD mice**

The novel object recognition (NOR) test was conducted to observe the impact of BME on the modified recognition memory caused by PD. The PD mice exhibited a significant decrease ( $P < 0.05$ ) in the time spent exploring novel objects compared to the control mice. The exploration time of the novel object significantly increased ( $P < 0.05$ ) in both pre- and post-treated mice compared to PD mice, as a result of the pre- and post-treatment with BME. Furthermore, the discrimination index of mice with Parkinson's disease was considerably reduced ( $P < 0.05$ ) compared to control mice. Both pre-treated and post-treated mice had significantly higher Discrimination index (DI) compared to PD mice (Fig. 3).

### **Effect of BME on the expression of AMPAR subunits GluR1 in the hippocampus of PD mice**

Quantitative Real-time PCR data showed a significant rise in the expression of GluR1-AMPA subunit mRNA in the hippocampus of mice with rotenone-induced Parkinson's disease, as compared to the control mice ( $P < 0.05$ ) whereas both pre- and post-treatment of PD animals with BME led to a significant reversal of its expression compared to that in the PD mice ( $P < 0.05$ ) (Fig. 4A). The western blot analysis demonstrated that treatment with BME significantly declined the elevated expression of the GluR1 subunit in PD mice ( $P < 0.05$ ) (Fig. 4B-C). Furthermore, immunofluorescence analysis of GluR1 indicates a significant increase in immunoreactivity in the DG, CA1, and CA3 regions of PD mice hippocampus compared to the control group mice. In the control group, most of the cells exhibited a consistent distribution and intensity of the GluR1 signal (Fig. 4D-I). In contrast, a significant reduction in immunoreactivity was found in the same areas of the hippocampus in PD mice as a result of both pre-

treatment and post-treatment with BME (Fig. 4D-I). However, the pre-BME treatment has a higher ameliorating potential than the post-BME treatment.

### **Effect of BME on the expression of AMPAR subunits GluR2 in the hippocampus of PD mice**

The quantitative RT-PCR investigation of the GluR2 subunit of the AMPA receptor mRNA expression in the hippocampus regions of PD mice showed a significantly reduced expression of GluR2-AMPA subunit mRNA compared to the control mice ( $P < 0.05$ ). Unlike the PD mice, the mice treated with BME, both before and after, exhibited a significant elevation in its expression ( $P < 0.05$ ) (Fig. 5A). However, there is a significant distinction between the two BME dosages, indicating that administering BME before PD has a more positive impact compared to administering it after PD symptoms. The western blot findings revealed a significant decrease in the expression of the GluR2 subunit compared to the control mice ( $P < 0.05$ ). Compared to PD mice, both the pre- and post-treated BME groups showed a significant increase in the expression of GluR2 (Fig. 5B-C). However, the pre-treatment resulted in a greater elevation in expression compared to the post-treatment of BME. Furthermore, like immunoblotting expression trends, the immunofluorescence examination of GluR2 reveals significantly reduced immunoreactivity in the DG, CA1, and CA3 regions of the PD mice hippocampus compared to the control group of mice. Conversely, both before and after treatment, BME significantly reduced immunoreactivity in the hippocampus regions of mice with Parkinson's disease (Fig. 5D-I). However, in this scenario, the pre-BME treatment exerts a significantly greater ameliorating potential than the post-BME treatment.

## **Effect of BME on the expression of trafficking proteins in the hippocampus of PD mice**

The western blotting of trafficking proteins showed that the expression of TARPY-2, PICK1 and PSD-95 were significantly higher in the PD mice than in the control group ( $P < 0.05$ ). Furthermore, TARPY-2, PICK1 and PSD-95 expression were significantly lower in the pre- and post-treated BME groups than in the mice with Parkinson's disease (PD). On the other hand, expression was lower following pre-treatment than following post-treatment BME (Fig. 6A-D).

### **Effect of BME on the expression of CREB and BDNF in the hippocampus of PD mice**

The Western blot analysis showed a significant decrease in the CREB and BDNF protein levels in the hippocampus of mice with rotenone-induced Parkinson's disease (PD) compared to the control group ( $P < 0.05$ ). However, pre-treatment with BME increased the CREB and BDNF protein levels ( $P < 0.05$ ), and the expression of CREB was found comparable to the control group. The upregulation of CREB and BDNF expression in post-BME treated PD mice was significantly higher, however, this amelioration was lesser compared to the pre-treatment condition (Fig. 7A-C).

## **Discussion**



This study specifically investigates the cognitive impairments caused by Parkinson's disease through changes in proteins related with synaptic plasticity. It also explores the potential of *Bacopa monnieri* extract (CDRI-08) in protecting and treating the brain by restoring these proteins. Rotenone is recognised for its ability to develop an effective model of Parkinson's disease (PD) by inhibiting complex-I of mitochondria and inducing neurodegeneration [37–38]. Thus, we developed a PD mouse model by administering rotenone subcutaneously and validated it by motor behaviour test. Parkinson's disease (PD) is characterised by motor impairment, including muscle weakness, sluggish or impaired movement, coordination difficulties, and poor body balance[39]. Our result indicates that PD mice have reduced grip strength and motor coordination, as evidenced by the observed symptoms (Fig. 1A&B). However, the administration of BME (CDRI-08) considerably improves these impairments. Nevertheless, pre-treatment of BME exhibits a more noticeable impact, indicating that the preventive influence of BME on motor symptoms holds greater potential than its therapeutic effect. The presence of Lewy bodies can serve as evidence for the occurrence of Parkinson's disease. Lewy bodies are formed by the accumulation of misfolded  $\alpha$ -Synuclein protein and are recognised as a characteristic feature of Parkinson's disease [2]. The accumulation of pathogenic  $\alpha$ -Synuclein protein leads to a decrease in synaptic proteins, neuronal excitability, and connectivity, ultimately resulting in neuronal death. Our work revealed that treatment with BME (CDRI-08) successfully decreased the heightened  $\alpha$ -Synuclein expression in the hippocampal subregions (DG, CA3, and CA1), restoring it to its normal levels (Fig. 2). The increased expression of  $\alpha$ -Synuclein has been associated with a decrease in memory [40], as evidenced by our recognition memory test employing NORT. In NOR, PD mice exhibited a reduction in the amount of time they spent exploring novel things and instead focused their attention on objects they were already familiar with (Fig. 3.B). In addition, they displayed an inability to distinguish between new objects that they had previously encountered (Fig. 3. C). Both doses of BME (CDRI-08) exhibit equivalent efficacy in enhancing the condition. The PD mice were further used for the analysis of synaptic plasticity-associated genes and proteins. The major players in the mechanism of synaptic plasticity are the AMPA and NMDA receptors [41]. Changes in the properties and quantity of AMPA receptor subunits have a notable impact on modifying synaptic plasticity, such as long-term potentiation (LTP), long-term depression (LTD), and homeostasis. The results obtained from our qRT-PCR, western blot, and immunofluorescence (IFC) experiments indicate that the expression levels of GluR1 and GluR2 subunits (Figs. 4 & 5) suggest that PD leads to significant increase in GluR1 subunit expression and a notable decrease in GluR2 subunit expression in the hippocampus and its subregions, including the dentate gyrus (DG), CA3, and CA1. The discovery indicates that the GluR1 subunit, responsible for facilitating the influx of  $\text{Ca}^{2+}$  ions, is more prevalent in the post-synaptic membrane in Parkinson's disease [42]. Consequently, these neurons are more prone to stimulation as a result of an increased influx of  $\text{Ca}^{2+}$  ions. Conversely, the GluR2 subunit-containing AMPA receptor, which is impermeable to  $\text{Ca}^{2+}$  ions are found at lower levels in the post-synaptic membrane in PD. Activation of the NMDA receptor due to this distinction can potentially amplify the post-synaptic current, resulting in neuronal toxicity and subsequent cell death. These alterations may be linked to the decrease in cognitive function and memory observed in PD mice. However, the BME (CDRI-08) effectively reversed the changes in the expression of these two subunits. Nevertheless, the pre-treatment of BME has a more significant impact compared to post-treatment, indicating its possible

neuroprotective effect through enhancing brain connectivity, communication, and signal transmission. The restoration process may be attributed to an enhancement in the mice's performance observed in the NOR test, which is related to recognition memory. The increase in GluR1 containing  $\text{Ca}^{2+}$  permeable AMPAR, causes the membrane to become more depolarised, leading in the activation of a greater number of NMDA receptors on the post-synaptic membrane. This leads to a rapid synaptic response[43–44],resulting in the development of excitotoxicity [45]. In addition, the expression of PICK1 was significantly increased in PD mice (Fig. 6). Elevated levels of PICK1 in neurons result in reduced levels in the presence of GluR2 on the cell surface, as PICK1 facilitates the internalization of AMPA receptors[46]. Thus, in Parkinson's disease (PD), the increased expression of PICK1 results in an accelerated uptake of AMPA receptors that contain GluR2, which are situated on the postsynaptic membrane. In addition, there is a higher abundance of AMPA receptors that contain GluR1 on the postsynaptic membrane. PSD-95 and TARPy-2 are two crucial proteins that play a role in stabilising the AMPA receptor on the cell membrane[47–48]. A significant increase in the expression of PSD-95 was seen in mice with Parkinson's disease compared to control mice. Moreover, there was a substantial increase in the expression of TARPy-2 in the PD mice. Nevertheless, the PD mice exhibited a restoration of normal levels of PSD-95 and TARPy-2 when they were administered BME in both pre and post treatment, (Fig. 6) Even so, the application of pre BME treatment had a much more pronounced impact on all three trafficking proteins in comparison to the application after treatment. The result indicated the interaction between PSD-95 and TARPy-2, as well as other members of the TARP family which establishes the connection to AMPA receptors. In addition, they interact with the PDZ domains of PSD-95 via their C-terminal domains. The connection between PSD-95 and TARPy-2 is believed to strengthen the stability of the receptors by linking them to PSD. The connection between TARPs and PSD-95 is crucial for the synaptic localization of AMPA receptors[49]. Consequently, the increased amounts of PSD-95 and TARPy-2 in PD suggest that the AMPA receptor persists at the post-synaptic membrane in PD and activates the NMDA receptor, leading to a continual influx of  $\text{Ca}^{2+}$  into the post-synaptic neurons. Recent investigations have indicated that the stimulation of extrasynaptic NMDA receptors containing GluN2B subunits leads to a persistent dephosphorylation of CREB, which is referred to as CREB shut-off [50]. As a result, CREB becomes transcriptionally inactive due to its fast dephosphorylation at serine 133 [51] the result indicates that an increase in  $\text{Ca}^{2+}$  permeable AMPA receptors can initiate NMDA downstream signalling, potentially leading to the activation of the CREB-shut-off pathway in Parkinson's disease. Consequently, this impedes the activation of genes associated with plasticity, such as BDNF, resulting in impaired synaptic function, synapse loss, and eventual cellular death. Our data on the expression of CREB and BDNF provide evidence for this notion, as we observe a decrease in their expression in PD (Fig. 7). This suggests that there is a disruption in synaptic plasticity, which in turn leads to cognitive impairment. In addition, the BME (CDRI-08) enhances the reduced levels of CREB and BDNF expression to the same degree in both pre- and post-treatment. This indicates that BME (CDRI-08) possesses both memory-enhancing and neurotherapeutic properties for cognitive impairment.

## Conclusion

The findings of this study provide an insight into a molecular cascade that links the impairment in motor behaviour and recognition memory that is caused by Parkinson's disease with the altered expression of the synaptic plasticity-related receptors (GluR1 and GluR2), trafficking and regulator proteins, leading to the excitotoxicity, and also downregulating the BDNF. Furthermore, both pre-and post-treatment with *Bacopa monnieri* extract-CDRI-08 have significantly recovered the PD-associated alterations by modulating the expression of AMPA receptors, trafficking proteins (TARPy-2, PSD-95 and PICK1) and CREB shut-off pathway, indicating its potent therapeutic effect as a nootropic drug in which pre-treatment approach is more promising.

## Declarations

### Acknowledgements

The authors are grateful to CAS and DST-FIST Level II programs, Department of Zoology, Central Discovery Centre under the SATHI Programs in Banaras Hindu University (BH) for Confocal microscopy facility and Interdisciplinary School of Life Sciences (ISLS), Banaras Hindu University (BHU) for real-time PCR. VG acknowledges University Grants Commission for CSIR-UGC JRF and SRF.

### Authors' Contributions

**Vartika Gupta:** Planned and carried out experiments, captured images, processed data, carried out statistical analysis of the result, and prepared draft manuscript.

**S. Prasad:** Generated funds, developed concept and planned experiment, Interpreted the results, Edited and finalized the manuscript.

### Funding

This work was supported by Institute of Eminence, BHU, Indian Council of Medical Research (ICMR), CSIR, BRNS, Govt. of India.

### Data Availability

The datasets analyzed during the study are available from the corresponding author upon reasonable request.

### Ethics Approval

The present study was performed according to the guidelines of the Committee for Control and Supervision of Experiments on Animals (CPCSEA), and the Institutional Animal Ethical Committee of Banaras Hindu University, Varanasi, approved all experimental procedures (Approval no.: BHU/DOZ/IAEC/2021-2022/007, Dated 15/02/2022).

### Consent to Participate

Not Applicable

## Consent for Publication

Not Applicable

## Competing Interests

The authors declare no competing interests.

## References

1. Tysnes, O. B., & Storstein, A. (2017). Epidemiology of Parkinson's disease. *Journal of neural transmission (Vienna, Austria: 1996)*, 124(8), 901–905. <https://doi.org/10.1007/s00702-017-1686-y>
2. Mehra, S., Sahay, S., & Maji, S. K. (2019).  $\alpha$ -Synuclein misfolding and aggregation: Implications in Parkinson's disease pathogenesis. *Biochimica et biophysica acta. Proteins and proteomics*, 1867(10), 890–908. <https://doi.org/10.1016/j.bbapap.2019.03.001>
3. Balestrino, R., & Schapira, A. H. V. (2020). Parkinson disease. *European journal of neurology*, 27(1), 27–42. <https://doi.org/10.1111/ene.14108>
4. Vidović, M., & Rikalovic, M. G. (2022). Alpha-Synuclein Aggregation Pathway in Parkinson's Disease: Current Status and Novel Therapeutic Approaches. *Cells*, 11(11), 1732. <https://doi.org/10.3390/cells11111732>
5. Aarsland, D., Batzu, L., Halliday, G. M., Geurtsen, G. J., Ballard, C., Ray Chaudhuri, K., & Weintraub, D. (2021). Parkinson disease-associated cognitive impairment. *Nature reviews. Disease primers*, 7(1), 47. <https://doi.org/10.1038/s41572-021-00280-3>
6. Aarsland, D., Creese, B., Politis, M., Chaudhuri, K. R., Ffytche, D. H., Weintraub, D., & Ballard, C. (2017). Cognitive decline in Parkinson disease. *Nature reviews. Neurology*, 13(4), 217–231. <https://doi.org/10.1038/nrneurol.2017.27>
7. Das, T., Hwang, J. J., & Poston, K. L. (2019). Episodic recognition memory and the hippocampus in Parkinson's disease: A review. *Cortex; a journal devoted to the study of the nervous system and behavior*, 113, 191–209. <https://doi.org/10.1016/j.cortex.2018.11.021>
8. Gomperts S. N. (2016). Lewy Body Dementias: Dementia With Lewy Bodies and Parkinson Disease Dementia. *Continuum (Minneapolis, Minn.)*, 22(2 Dementia), 435–463. <https://doi.org/10.1212/CON.0000000000000309>
9. Sezgin, M., Bilgic, B., Tinaz, S., & Emre, M. (2019). Parkinson's Disease Dementia and Lewy Body Disease. *Seminars in neurology*, 39(2), 274–282. <https://doi.org/10.1055/s-0039-1678579>
10. Lu, B., Nagappan, G., & Lu, Y. (2014). BDNF and synaptic plasticity, cognitive function, and dysfunction. *Handbook of experimental pharmacology*, 220, 223–250. [https://doi.org/10.1007/978-3-642-45106-5\\_9](https://doi.org/10.1007/978-3-642-45106-5_9)

11. Magee, J. C., & Grienberger, C. (2020). Synaptic Plasticity Forms and Functions. *Annual review of neuroscience*, *43*, 95–117. <https://doi.org/10.1146/annurev-neuro-090919-022842>
12. Malenka, R. C., & Bear, M. F. (2004). LTP and LTD: an embarrassment of riches. *Neuron*, *44*(1), 5–21. <https://doi.org/10.1016/j.neuron.2004.09.012>
13. Diering, G. H., & Huganir, R. L. (2018). The AMPA Receptor Code of Synaptic Plasticity. *Neuron*, *100*(2), 314–329. <https://doi.org/10.1016/j.neuron.2018.10.018>
14. Effendy, M. A., Yunusa, S., Mat, N. H., Has, A. T. C., Müller, C. P., & Hassan, Z. (2023). The role of AMPA and NMDA receptors in mitragynine effects on hippocampal synaptic plasticity. *Behavioural brain research*, *438*, 114169. <https://doi.org/10.1016/j.bbr.2022.114169>
15. Di Maio, V., Ventriglia, F., & Santillo, S. (2016). AMPA/NMDA cooperativity and integration during a single synaptic event. *Journal of computational neuroscience*, *41*(2), 127–142. <https://doi.org/10.1007/s10827-016-0609-5>
16. Qu, W. R., Sun, Q. H., Liu, Q. Q., Jin, H. J., Cui, R. J., Yang, W., Song, B., & Li, B. J. (2020). Role of CPEB3 protein in learning and memory: new insights from synaptic plasticity. *Aging*, *12*(14), 15169–15182. <https://doi.org/10.18632/aging.103404>
17. Hollmann, M., & Heinemann, S. (1994). Cloned glutamate receptors. *Annual review of neuroscience*, *17*, 31–108. <https://doi.org/10.1146/annurev.ne.17.030194.000335>
18. Passafaro, M., Piëch, V., & Sheng, M. (2001). Subunit-specific temporal and spatial patterns of AMPA receptor exocytosis in hippocampal neurons. *Nature neuroscience*, *4*(9), 917–926. <https://doi.org/10.1038/nn0901-917>
19. Dingledine, R., Borges, K., Bowie, D., & Traynelis, S. F. (1999). The glutamate receptor ion channels. *Pharmacological reviews*, *51*(1), 7–61.
20. Leal, G., Comprido, D., & Duarte, C. B. (2014). BDNF-induced local protein synthesis and synaptic plasticity. *Neuropharmacology*, *76 Pt C*, 639–656. <https://doi.org/10.1016/j.neuropharm.2013.04.005>
21. Takeda, H., Kitaoka, Y., Hayashi, Y., Kumai, T., Munemasa, Y., Fujino, H., Kobayashi, S., & Ueno, S. (2007). Calcium/calmodulin-dependent protein kinase II regulates the phosphorylation of CREB in NMDA-induced retinal neurotoxicity. *Brain research*, *1184*, 306–315. <https://doi.org/10.1016/j.brainres.2007.09.055>
22. Sumathy, T., Govindasamy, S., Balakrishna, K., & Veluchamy, G. (2002). Protective role of Bacopa monniera on morphine-induced brain mitochondrial enzyme activity in rats. *Fitoterapia*, *73*(5), 381–385. [https://doi.org/10.1016/s0367-326x\(02\)00114-4](https://doi.org/10.1016/s0367-326x(02)00114-4)
23. Banerjee, S., Anand, U., Ghosh, S., Ray, D., Ray, P., Nandy, S., Deshmukh, G. D., Tripathi, V., & Dey, A. (2021). Bacosides from Bacopa monnieri extract: An overview of the effects on neurological disorders. *Phytotherapy research : PTR*, *35*(10), 5668–5679. <https://doi.org/10.1002/ptr.7203>
24. Pathak, A., Kulshreshtha, D. K., & Maurya, R. (2005). Chemical constituents of Bacopa procumbens. *Natural product research*, *19*(2), 131–136. <https://doi.org/10.1080/14786410410001704732>

25. Ohta, T., Nakamura, S., Nakashima, S., Oda, Y., Matsumoto, T., Fukaya, M., Yano, M., Yoshikawa, M., & Matsuda, H. (2016). Chemical structures of constituents from the whole plant of *Bacopa monniera*. *Journal of natural medicines*, *70*(3), 404–411. <https://doi.org/10.1007/s11418-016-0986-0>
26. Aguiar, S., & Borowski, T. (2013). Neuropharmacological review of the nootropic herb *Bacopa monnieri*. *Rejuvenation research*, *16*(4), 313–326. <https://doi.org/10.1089/rej.2013.1431>
27. Jeyasri, R., Muthuramalingam, P., Adarshan, S., Shin, H., & Ramesh, M. (2022). Assessing the Anti-inflammatory Effects of *Bacopa*-Derived Bioactive Compounds Using Network Pharmacology and *In Vitro* Studies. *ACS omega*, *7*(44), 40344–40354. <https://doi.org/10.1021/acsomega.2c05318>
28. Srivastav, S., Fatima, M., & Mondal, A. C. (2017). Important medicinal herbs in Parkinson's disease pharmacotherapy. *Biomedicine & pharmacotherapy = Biomedecine&pharmacotherapie*, *92*, 856–863. <https://doi.org/10.1016/j.biopha.2017.05.137>
29. Singh, B., Pandey, S., Verma, R., Ansari, J. A., & Mahdi, A. A. (2016). Comparative evaluation of extract of *Bacopa monnieri* and *Mucuna pruriens* as neuroprotectant in MPTP model of Parkinson's disease. *Indian journal of experimental biology*, *54*(11), 758–766.
30. Shiotsuki, H., Yoshimi, K., Shimo, Y., Funayama, M., Takamatsu, Y., Ikeda, K., Takahashi, R., Kitazawa, S., & Hattori, N. (2010). A rotarod test for evaluation of motor skill learning. *Journal of neuroscience methods*, *189*(2), 180–185. <https://doi.org/10.1016/j.jneumeth.2010.03.026>
31. Barman, B., Kushwaha, A., & Thakur, M. K. (2021). Vitamin B<sub>12</sub>-folic acid supplementation regulates neuronal immediate early gene expression and improves hippocampal dendritic arborization and memory in old male mice. *Neurochemistry international*, *150*, 105181. <https://doi.org/10.1016/j.neuint.2021.105181>
32. Bradford M. M. (1976). A rapid and sensitive method for the quantitation of microgram quantities of protein utilizing the principle of protein-dye binding. *Analytical biochemistry*, *72*, 248–254. <https://doi.org/10.1006/abio.1976.9999>
33. Singh, K., Gaur, P., & Prasad, S. (2007). Fragile x mental retardation (Fmr-1) gene expression is down regulated in brain of mice during aging. *Molecular biology reports*, *34*(3), 173–181. <https://doi.org/10.1007/s11033-006-9032-8>
34. Gaur, P., & Prasad, S. (2014). Alterations in the Sp1 binding and Fmr-1 gene expression in the cortex of the brain during maturation and aging of mouse. *Molecular biology reports*, *41*(10), 6855–6863. <https://doi.org/10.1007/s11033-014-3571-1>
35. Rao, X., Huang, X., Zhou, Z., & Lin, X. (2013). An improvement of the 2<sup>-ΔΔCT</sup> method for quantitative real-time polymerase chain reaction data analysis. *Biostatistics, bioinformatics and biomathematics*, *3*(3), 71–85.
36. Dalvi PS, Belsham DD. Immunofluorescence of GFAP and TNF-α in the Mouse Hypothalamus. *Bio Protoc.* 2021 Jul 5;11(13):e4078. doi: 10.21769/BioProtoc.4078.
37. Thakur, P., & Nehru, B. (2014). Modulatory effects of sodium salicylate on the factors affecting protein aggregation during rotenone induced Parkinson's disease pathology. *Neurochemistry international*, *75*, 1–10. <https://doi.org/10.1016/j.neuint.2014.05.002>

38. Konnova, E. A., & Swanberg, M. (2018). Animal Models of Parkinson's Disease. In T. B. Stoker (Eds.) et. al., *Parkinson's Disease: Pathogenesis and Clinical Aspects*. Codon Publications.
39. Simon, D. K., Tanner, C. M., & Brundin, P. (2020). Parkinson Disease Epidemiology, Pathology, Genetics, and Pathophysiology. *Clinics in geriatric medicine*, 36(1), 1–12.  
<https://doi.org/10.1016/j.cger.2019.08.002>
40. Volpicelli-Daley, L. A., Luk, K. C., Patel, T. P., Tanik, S. A., Riddle, D. M., Stieber, A., Meaney, D. F., Trojanowski, J. Q., & Lee, V. M. (2011). Exogenous  $\alpha$ -Synuclein fibrils induce Lewy body pathology leading to synaptic dysfunction and neuron death. *Neuron*, 72(1), 57–71.  
<https://doi.org/10.1016/j.neuron.2011.08.033>.
41. Diering, G. H., & Huganir, R. L. (2018). The AMPA Receptor Code of Synaptic Plasticity. *Neuron*, 100(2), 314–329. <https://doi.org/10.1016/j.neuron.2018.10.018>, Jourdi, H., & Kabbaj, M. (2013). Acute BDNF treatment upregulates GluR1-SAP97 and GluR2-GRIP1 interactions: implications for sustained AMPA receptor expression. *PloS one*, 8(2), e57124. <https://doi.org/10.1371/journal.pone.0057124> ).
42. Burnashev, N., Monyer, H., Seeburg, P. H., & Sakmann, B. (1992). Divalent ion permeability of AMPA receptor channels is dominated by the edited form of a single subunit. *Neuron*, 8(1), 189–198.  
[https://doi.org/10.1016/0896-6273\(92\)90120-3](https://doi.org/10.1016/0896-6273(92)90120-3),
43. Deng, Y. P., Xie, J. P., Wang, H. B., Lei, W. L., Chen, Q., & Reiner, A. (2007). Differential localization of the GluR1 and GluR2 subunits of the AMPA-type glutamate receptor among striatal neuron types in rats. *Journal of chemical neuroanatomy*, 33(4), 167–192.  
<https://doi.org/10.1016/j.jchemneu.2007.02.008>
44. Essin, K., Nistri, A., & Magazanik, L. (2002). Evaluation of GluR2 subunit involvement in AMPA receptor function of neonatal rat hypoglossal motoneurons. *The European journal of neuroscience*, 15(12), 1899–1906. <https://doi.org/10.1046/j.1460-9568.2002.02045.x>
45. Lau, A., & Tymianski, M. (2010). Glutamate receptors, neurotoxicity and neurodegeneration. *Pflugers Archiv : European journal of physiology*, 460(2), 525–542. <https://doi.org/10.1007/s00424-010-0809-1>
46. Perez, J. L., Khatri, L., Chang, C., Srivastava, S., Osten, P., & Ziff, E. B. (2001). PICK1 targets activated protein kinase Calpha to AMPA receptor clusters in spines of hippocampal neurons and reduces surface levels of the AMPA-type glutamate receptor subunit 2. *The Journal of neuroscience : the official journal of the Society for Neuroscience*, 21(15), 5417–5428.  
<https://doi.org/10.1523/JNEUROSCI.21-15-05417.2001>
47. Hastie, P., Ulbrich, M. H., Wang, H. L., Arant, R. J., Lau, A. G., Zhang, Z., Isacoff, E. Y., & Chen, L. (2013). AMPA receptor/TARP stoichiometry visualized by single-molecule subunit counting. *Proceedings of the National Academy of Sciences of the United States of America*, 110(13), 5163–5168.  
<https://doi.org/10.1073/pnas.1218765110>,
48. Tomita, S., Stein, V., Stocker, T. J., Nicoll, R. A., & Brecht, D. S. (2005). Bidirectional synaptic plasticity regulated by phosphorylation of stargazin-like TARPs. *Neuron*, 45(2), 269–277.  
<https://doi.org/10.1016/j.neuron.2005.01.0092000>, Tomita et al., 2005

49. Ravi, A. S., Zeng, M., Chen, X., Sandoval, G., Diaz-Alonso, J., Zhang, M., & Nicoll, R. A. (2022). Long-term potentiation reconstituted with an artificial TARP/PSD-95 complex. *Cell reports*, *41*(2), 111483. <https://doi.org/10.1016/j.celrep.2022.111483>
50. Grochowska, K. M., Bär, J., Gomes, G. M., Kreutz, M. R., & Karpova, A. (2021). Jacob, a Synapto-Nuclear Protein Messenger Linking N-methyl-D-aspartate Receptor Activation to Nuclear Gene Expression. *Frontiers in synaptic neuroscience*, *13*, 787494. <https://doi.org/10.3389/fnsyn.2021.787494>
51. Mohanan, A. G., Gunasekaran, S., Jacob, R. S., & Omkumar, R. V. (2022). Role of Ca<sup>2+</sup>/Calmodulin-Dependent Protein Kinase Type II in Mediating Function and Dysfunction at Glutamatergic Synapses. *Frontiers in molecular neuroscience*, *15*, 855752. <https://doi.org/10.3389/fnmol.2022.855752>

## Figures



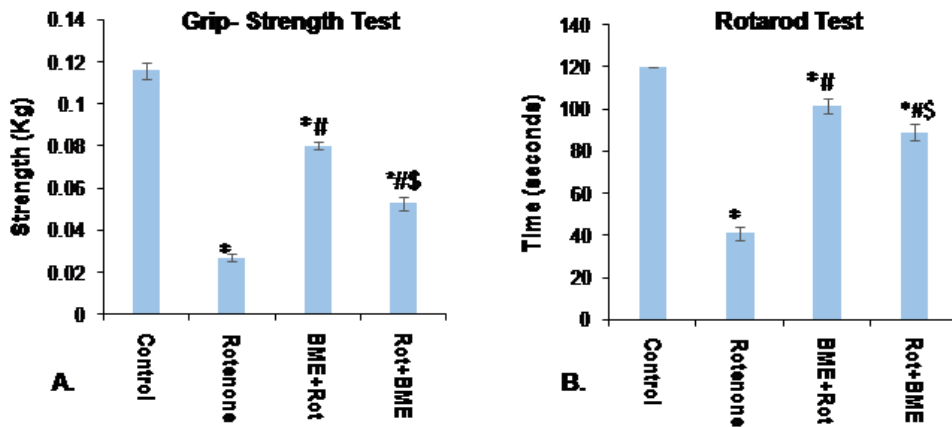


**Figure 1**

Effects of BME (CDRI-08) on the motor coordination in Vehicle treated control, Rotenone- treated (PD), pre-BME treated PD-mice (BME+Rot) and post-BME treated PD-mice (Rot+BME). Grip strength (Kg) (A); Latency time to fall (Sec) of mice on the Rotarod (B). Data present mean  $\pm$  SEM; \*, a significant difference ( $p < 0.05$ ) between control and other groups; #, a significant difference ( $p < 0.05$ ) between Rotenone and BME groups; \$, significant difference ( $p < 0.05$ ) between BME+Rot and Rot+BME groups.

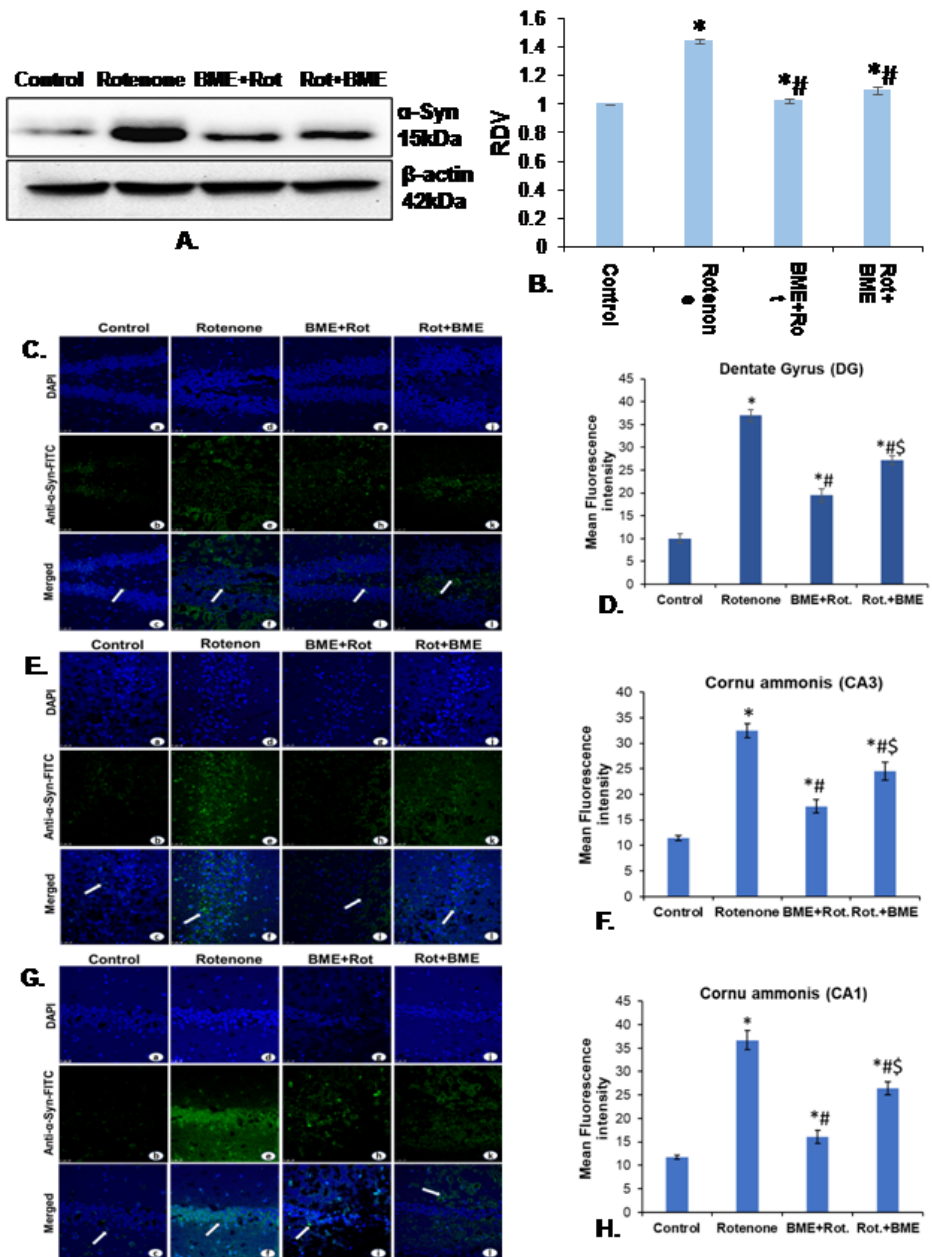


**Figure 2**

Effects of BME (CDRI-08) on the expression of the  $\alpha$ -Synuclein protein in the hippocampus of Vehicle treated control, rotenone-treated (PD), pre-BME treated PD-mice (BME+Rot) and post-BME treated PD-mice (Rot+BME). Western blot analysis of  $\alpha$ -Synuclein and  $\beta$ -actin (A). Histogram represents RDV of  $\alpha$ -Synuclein (IDV of  $\alpha$ -Synuclein /IDV of  $\beta$ -actin) (B); Photomicrographs show immunofluorescence illustrating FITC-labelled signals of  $\alpha$ -Synuclein in DG (C), CA3 (E), and CA1 (G) region of the

hippocampus; Histogram represent mean fluorescence intensity of DG (D), CA3 (F), and CA1 (H) regions of hippocampus. Data represent mean  $\pm$  SEM; \*, a significant difference ( $p < 0.05$ ) between control and other groups; #, a significant difference ( $p < 0.05$ ) between rotenone and BME groups; \$, significant difference ( $p < 0.05$ ) between BME+Rot and Rot+BME groups.

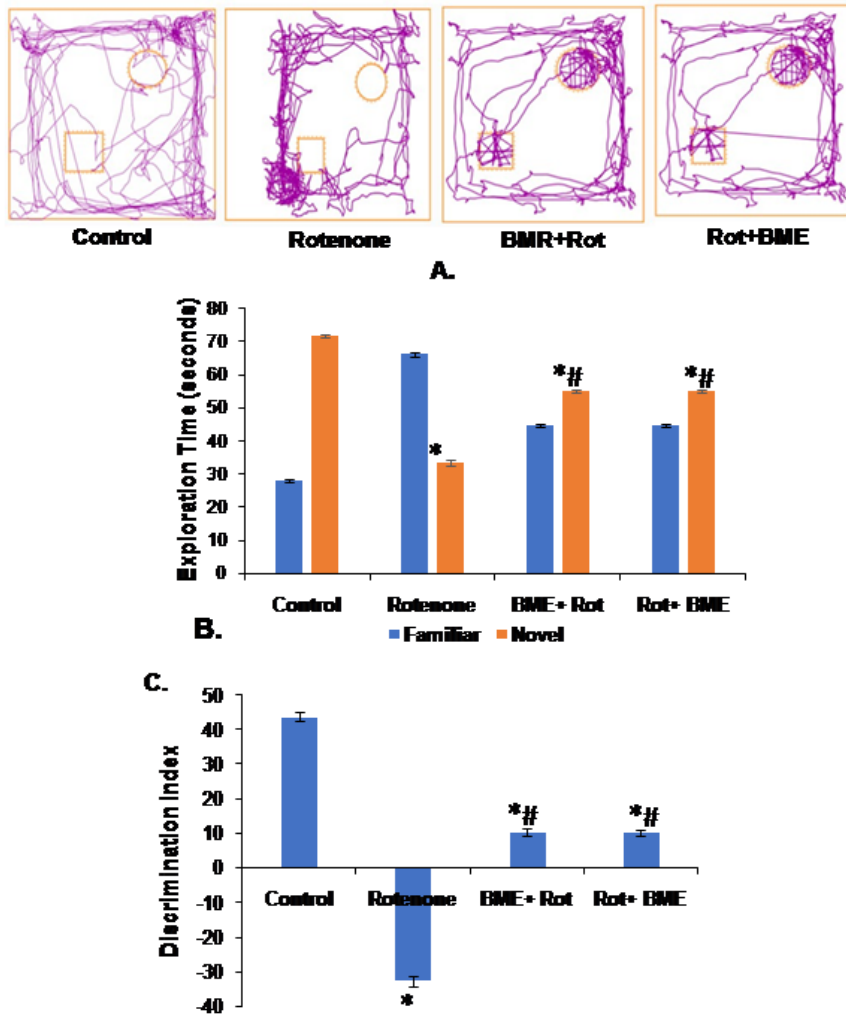
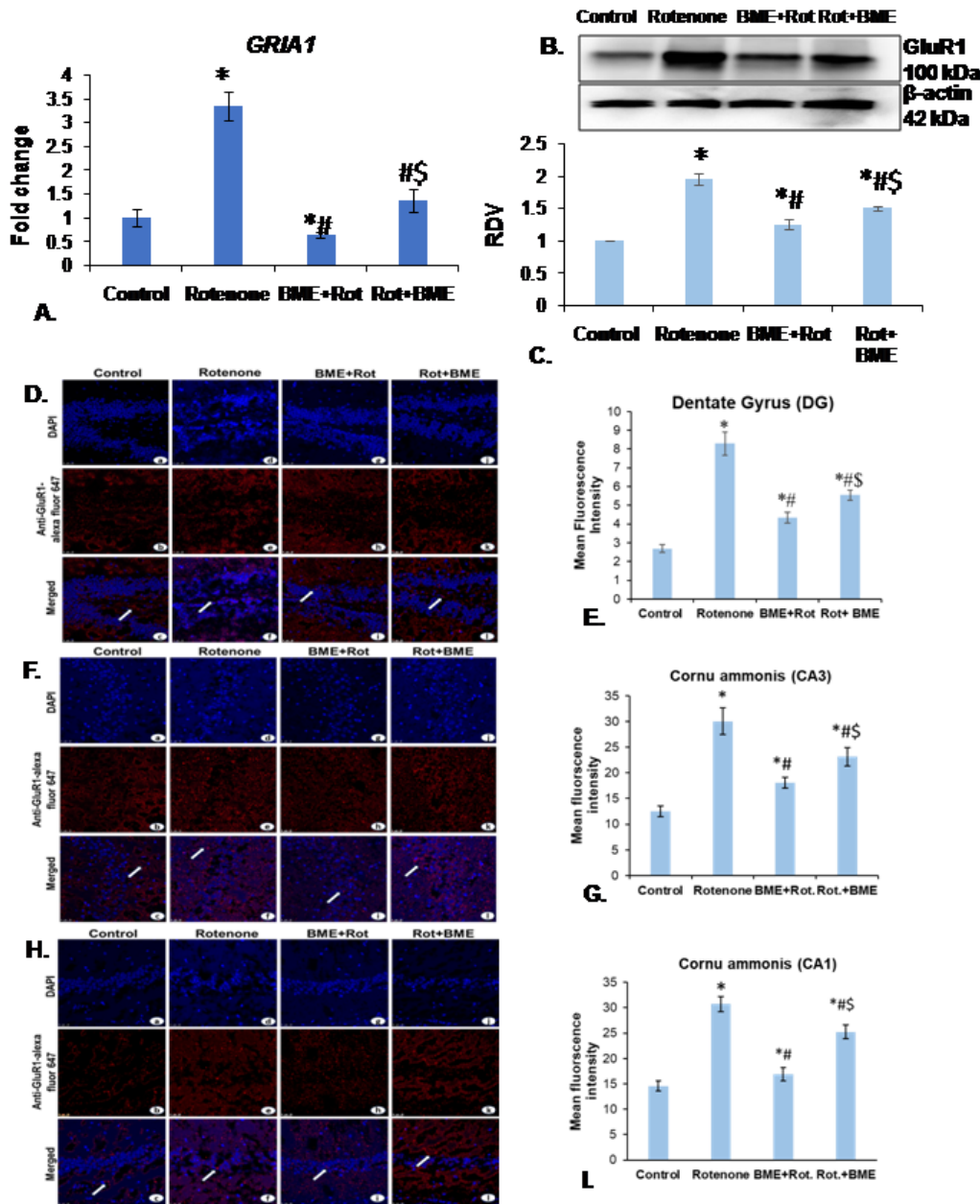


Figure 3

Effect of BME (CDRI-08) on recognition memory of vehicle treated control, Rotenone-treated (PD), pre-BME treated PD-mice and post-BME treated PD-mice. Track plot of mice in novel object recognition test box (A); Time spent (Sec) by mice with novel and familiar objects (B); Discrimination index (C) Data represent mean  $\pm$  SEM; \*, significant difference ( $p < 0.05$ ) between control and other groups; #, significant difference ( $p < 0.05$ ) between BME+rotenone and BME groups; \$, significant difference ( $p < 0.05$ ) between BME+Rot and Rot+BME groups.



## Figure 4

Effects of BME (CDRI-08) on the expression of GluR1 AMPA receptor subunit in the hippocampus of vehicle treated control, Rotenone-treated (PD), pre-BME treated PD-mice (BME+Rot) and post-BME treated PD-mice (Rot+BME). Histograms represent fold change of GluR1 (*GRIA-1*) mRNA level (A); Western blot of GluR1 and  $\beta$ -actin (B). Histogram representing RDV of GluR1 (IDV of GluR1 /IDV of  $\beta$ -actin) (C); Photomicrographs show immunofluorescence showing TRITC-labelled signals of GluR1 in DG (D), CA3 (F), and CA1 (H) regions of hippocampus; Histograms represent mean fluorescence intensity of DG (E), CA3 (G), and CA1 (I) regions of hippocampus. Data represent mean  $\pm$  SEM; \*, a significant difference ( $p < 0.05$ ) between control and other groups; #, a significant difference ( $p < 0.05$ ) between Rotenone (PD) and BME groups; \$, significant difference ( $p < 0.05$ ) between BME+Rot and Rot+BME groups.

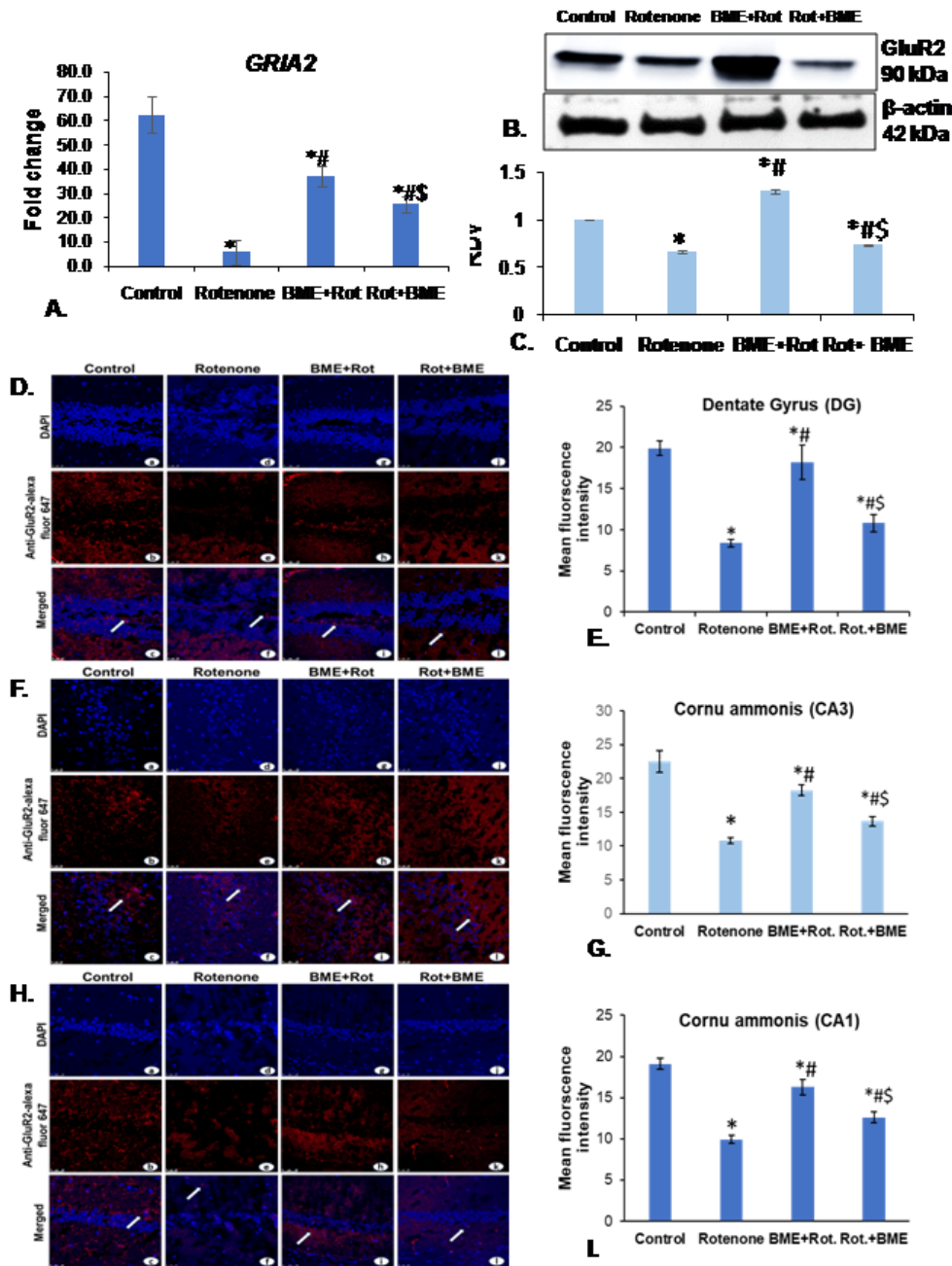


**Figure 5**

Effect of BME (CDRI-08) on the expression of GluR2 in the hippocampus of Vehicle-treated control, Rotenone-treated (PD), pre-BME treated PD-mice (BME+Rot) and post-BME treated PD-mice (Rot+BME). Histograms represent fold change in the level of GluR2 (*GRIA-2*) mRNA expression (A); Western blot of GluR2 and  $\beta$ -actin (B). Histograms represent RLV of GluR2 (IDV of GluR2 /IDV of  $\beta$ -actin) (C); Photomicrographs show immunofluorescence illustrating TRITC-labelled signals of GluR1 in DG (D), CA3

(F), and CA1 (H) region of hippocampus; Histogram representing mean fluorescence intensity of DG (E), CA3 (G), and CA1 (I) region of hippocampus. Data represent mean  $\pm$  SEM; \*, a significant difference ( $p < 0.05$ ) between control and other groups; #, a significant difference ( $p < 0.05$ ) between Rotenone and BME groups; \$, significant difference ( $p < 0.05$ ) between BME+Rot and Rot+BME groups.

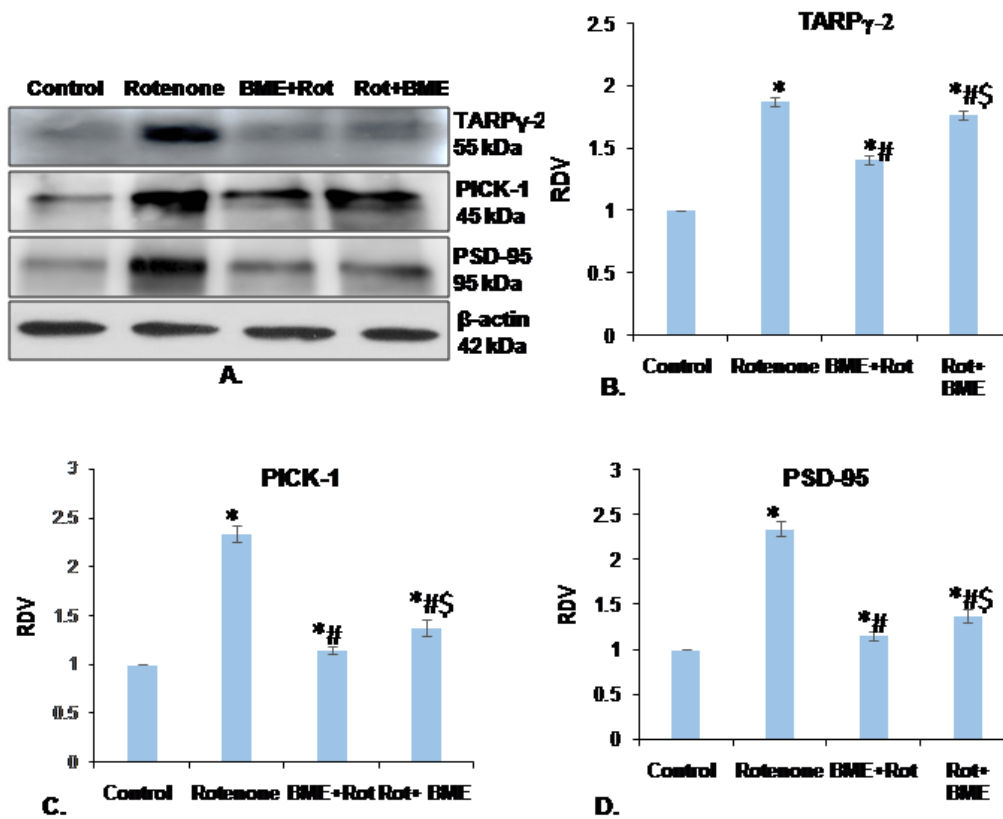
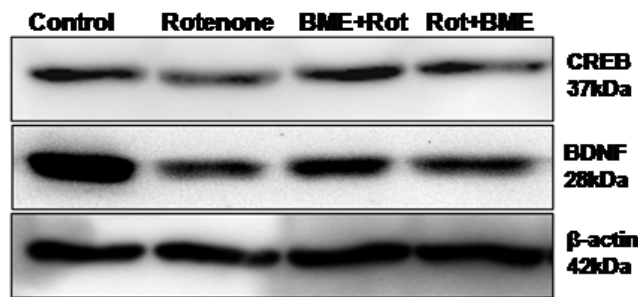
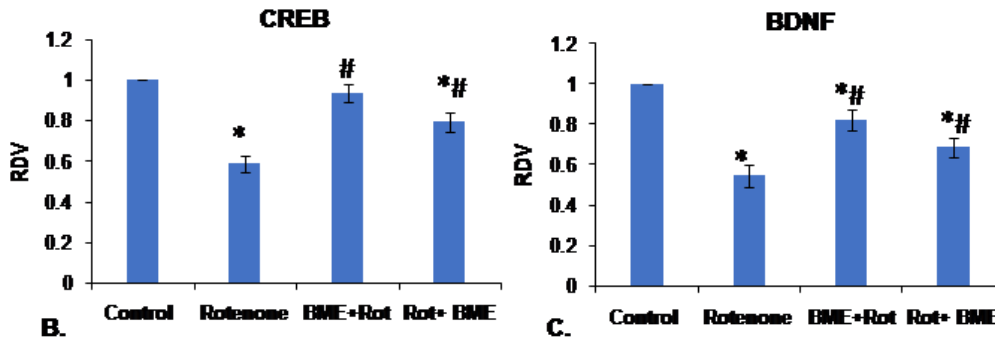


Figure 6

Effects of BME (CDRI-08) on the expression of trafficking proteins of AMPAR in the hippocampus of Vehicle treated Control, Rotenone-treated (PD), pre-BME treated PD-mice (BME+Rot) and post-BME treated PD-mice (Rot+BME). Western blot of TAR $\gamma$ -2, PICK-1, PSD-95, and  $\beta$ -actin (A). Histograms represent iRDV of TAR $\gamma$ -2, PICK-1, and PSD-95 (IDV of TAR $\gamma$ -2, PICK-1, PSD-95 /IDV of  $\beta$ -actin) (B, C and D). Data represent mean  $\pm$  SEM; \*, a significant difference ( $p < 0.05$ ) between control and other groups; #, a significant difference ( $p < 0.05$ ) between rotenone and BME groups; \$, significant difference ( $p < 0.05$ ) between BME+Rot and Rot+BME groups.



**A.**





## Figure 7

Effects of BME (CDRI-08) on the expression of CREB and BDNF in the hippocampus of Vehicle treated control, Rotenone-treated (PD), pre-BME treated PD-mice (BME+Rot) and post-BME treated PD-mice (Rot+BME). Western blot of CREB, BDNF, and  $\beta$ -actin (A). Histograms represent RDV of CREB and BDNF (IDV of CREB, BDNF /IDV of  $\beta$ -actin) (B and C). Data present mean  $\pm$  SEM; \*, a significant difference ( $p < 0.05$ ) between control and other groups; #, a significant difference ( $p < 0.05$ ) between rotenone and BME groups.